

# NUMERICAL DYNAMIC SIMULATIONS FOR THE PREDICTION OF DAMAGE AND LOSS OF CAPACITY OF RC COLUMN SUBJECTED TO CONTACT DETONATIONS

MAGALI ARLERY\*, ALAIN ROUQUAND AND SEREY CHHIM

CEA, DAM, GRAMAT, F-46500 Gramat, France

\* e-mail: magali.arlery-genetier@cea.fr

**Keywords:** RC column, Contact detonations, Numerical simulation, Damage criterion, Analytical formula

**Abstract:** The assessment of dynamic response and residual capacity of reinforced concrete (RC) columns to blast load is decisive for protection of buildings, especially regarding progressive collapse risk. In the case of explosive devices placed next to a critical structural element, complex and extreme loading is applied on the nearby system and the material response is characterized by high non-linearities. In this study, detailed weak-coupled fluid dynamics and finite element calculations are first used to investigate several scenarios of blast loading and RC columns response for contact detonations from 2.5 kg to 500 kg in a generic building. A general damage criterion is proposed and numerically evaluated in terms of residual axial load-carrying capacity. Parametric studies using a simplified loading methodology are then carried out to investigate the influence of charge weight, stand-off distance, column dimensions and concrete strength. Based on these results, an analytical empirical formula is derived to predict the damage level of the column.

## 1 INTRODUCTION

Bombing is a threat with low probability but with disastrous consequences. Accidental or intentional events that have damaged important infrastructures in recent years have focused attention of constructive guidelines and research community on blast loads effects. Structural damages caused by blast loading are the combination of both immediate effects and consecutive hazards, among which progressive collapse. This catastrophic failure mode occurs when the initial failure of one or several key load-carrying members gives rise to a more widespread failure of the surrounding members, up to complete or disproportionately large collapse of the whole structure. The limitations of progressive collapse analysis procedures prescribed by the US General Service Administration (GSA) [1] and the US

Department of Defense (DoD) [2] have been largely discussed, [3-6]. In particular, it has been demonstrated by Shi *et al.* [6] that considering and quantifying the direct damage of all structural components affected by the blast can improve the alternate load path method proposed by the guidelines. Therefore, one of the most useful information when assessing the consequences of a blast event on a building would be the accurate evaluation of dynamic response and residual load-carrying capacity of the primary supporting members. Pressure-impulse (P-I) diagrams based on a simplified single degree of freedom (SDOF) models are commonly used to assess the response of a component to a particular load history, including blast loads. However, even if some works, [7-9], attempted to include noticeable details in the analysis, such as the irregular pulse loading shape and/or the non-

linear resistance function of the element, such analysis might not be suitable for loading conditions imposed by close-in detonations. In that case, the structure damage is primarily governed by response at local modes and detailed numerical simulations have to be done. Shi *et al.* [10] calculated with LS-DYNA the response of RC columns to an idealized triangular blast load uniformly applied to the front face in order to establish (P-I) diagrams and analytical formulas for the asymptotes. Even if the simplification in loading description is consistent with the prescription of the commonly used Technical Manual TM5-1300 [11], it is no more suitable when the charge is very close to the column because load becomes strongly non uniform. Wu *et al.* [12] carried out similar investigations using the Arbitrary Lagrange-Euler solver of LS-DYNA for a charge of 25 kg TNT detonating in front of different columns. In both studies, the residual axial load capacity is considered as the most relevant criterion to quantify the damage of the column after the blast. In fact, this criterion is independent on damage modes, unlike the maximum deflection criteria commonly used in SDOF analyses, and inhomogeneous local properties, such as strength material reduction or crater dimensions.

The present study is part of the European project SPIRIT (Safety and Protection of built Infrastructures to Resist Integral Threat) which attempt to develop an integrated approach to mitigate chemical, biological, radiological and explosive threats to built infrastructures. Considering the explosive threat, part of the work consists in developing methodologies to quantify the consequences of attack in terms of structural damage at both local and global levels. Local damages directly induced by blast on primary structural components are, in a first step, numerically assessed on columns for several scenarios of attacks on a generic 17-floors building designed in accordance with European regulations. In a second step, the numerical analysis is broadened to parametric studies on loading and structural parameters. The results are used to propose an analytical formula for the prediction of the damage level.

Blast loads investigated are distinguished by close-in (5 cm) to near field (1 m) detonations and a large weight range (2.5 to 500 kg TNT). Special care is taken in the adopted numerical methodology to accurately calculate the non-uniform and irregular blast load applied on all surfaces of the structure and to capture the complete response of the component. Comparisons between experimental results and empirical formula used in constructive guidelines are done to validate different parts of the developed methodology.

## 2 NUMERICAL ANALYSIS

### 2.1 Geometries, elements and boundaries

Figure 1 shows an example of a finite element model representing a RC column in the generic building and the explosive device. The explosive charge is supposed to be spherical and placed on the floor, at the bottom of the column. The meshes are composed of 3D 8-nodes brick elements with a single integration point for the concrete volume and of 1D beam elements for the reinforcing steel bars. Perfect bonds are assumed between the two materials. A mesh size of 1.5 cm is typically used.

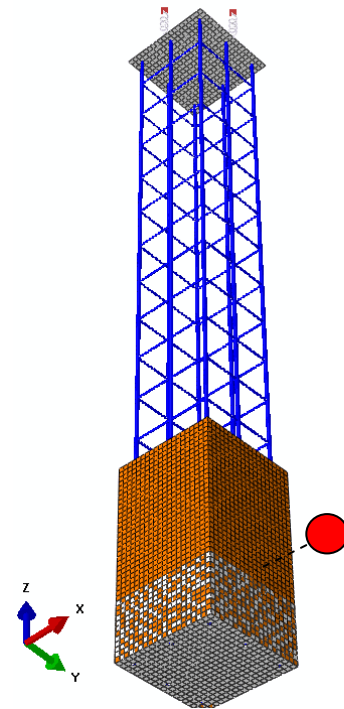


Figure 1: Finite element model of a RC column

For models including nearby structural components of the columns, a perfect tie is assumed between the connecting surfaces. The top face of the column is constrained against horizontal motions. The bottom face (1 m above the floor) is constrained against vertical motion and also against the three rotations. The vertical borders of the slab are constrained against horizontal motions and against rotations.

For parametric studies, only a single column is represented in the FEM model. In that case, a footing and a head are included in the numerical model, which constitute rigid bodies that simulate the connexions of the column with the floor and the roof. The slabs thickness is supposed to be 30 cm. Preliminary tests proved that free rotations at the footing lead to non realistic behaviour for close-in detonation, with too large rotation of the column end. In fact, even if for design considerations under gravity and service loads, the column boundary condition at the lower column end is generally taken as a pinned link, which is the most appropriate to simulate low strains and low rotations at the floor junction level, these conditions are not satisfied for close-in detonations. Consequently, embedded conditions in the floor are supposed for all numerical simulations on single columns. However, as the connexion between the upper part of the column and the roof is far from the loaded area, standard assumptions are used: fixed displacements and possible rotations in the x- and y-direction, with stiffness modelled by four linear springs generating a resisting momentum proportional to the rotation angle  $\theta$  of the column.

Steel reinforcement consists in longitudinal rods and transverse hoops. In the generic building columns have decreasing cross-sections from basement to upper levels with variable number (4 to 8) and diameters (12 to 28 mm) of longitudinal bars, as well as variable diameters (6 to 12 mm) and partition distances (14 to 30 cm) of transverse hoops. For single columns of the parametric study, reinforcement consists in 8 or 12 longitudinal bars for respectively square or rectangular

sections, with a cross area equal to 1% of the concrete area. Transverse reinforcements are positioned 25 cm part along the vertical direction and have a mass equal to 1/3 of the mass of longitudinal reinforcement.

## 2.2 Material models

The concrete behaviour is simulated with the material model PRM, developed by Pontiroli, Rouquand and Mazard [13]. This model has been used to simulate a wide range of problems from quasi-static configurations to high dynamic impacts or blast loading on complex reinforced concrete structures. Two versions of the model are available: the two-scalar damage model and the two-scalar damage model coupled with the Krieg [14] and Swenson [15] plasticity model. The coupled version includes mechanisms occurring at high pressure levels: pore compaction, shear plastic limit evolution and water content effects. As these mechanisms do not play a significant role in the material response for blast loadings considered in the present study and are computing process time consuming, the two-scalar damage model is used. While not a material property, an erosion criterion is introduced in the calculation so that elements are suppressed from the analysis when their maximal tensile strain reaches 50 %.

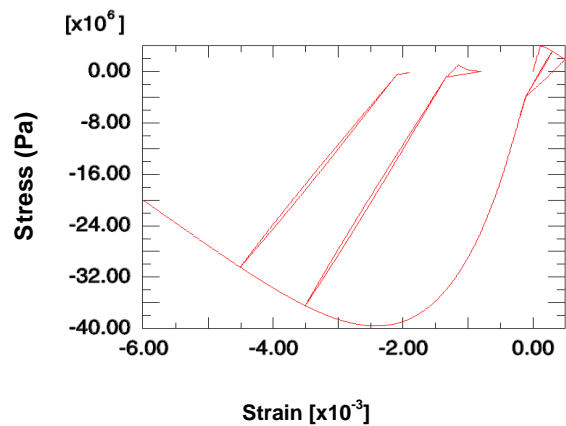


**Figure 2:** Stress-strain relation in concrete for cyclic tensile and compressive load

Figure 2 shows a typical stress-strain relation for cyclic tensile or compressive loadings given by the two-scalar damage

model. The following main physical mechanisms are taken into account: (i) crack closure effect observed during a tensile then compressive loading; (ii) strain rate effects on compressive and tensile strengths with constancy of fracture energy; (iii) irreversible strains generated for tensile or compressive loading; (iv) friction mechanism responsible for hysteretic loops during cyclic loading; (v) dissipation of a constant energy when a localized crack propagates in the mesh ensured by the Hillerborg [16] regularisation technique.

Steel behaviour is simulated with the Johnson Cook dynamic failure model. This model includes an isotropic hardening mechanism with strain rate dependency and a damage mechanism that simulates the progressive failure of the reinforcement. Static yield stress is taken equal to 500 MPa. The failure process starts when the plastic strain reaches 10% and the complete failure is achieved for plastic strains higher than 12.5%.

### 2.3 Analytical procedure

The adopted analytical procedure includes the following successive calculations.

#### Stage 1: preload

The compressive axial preload due to gravity in a low-to-high rise buildings can have a significant influence on the column behaviour under blast. Therefore an initial axial force equal to 25% of the compressive concrete strength is prescribed and, furthermore, the action line of this force is brought out of centre to take into account eccentricity. This eccentricity is taken equal to the column height divided by 400. The force must be applied gradually due to the explicit scheme of the analysis: a duration of 50 ms is used.

#### Stage 2: blast load

Blast load is calculated with the Eulerian solver of the OURANOS code [17], from detonation time to a few milliseconds, with the

assumption that the structure is perfectly rigid. In the numerical model, air is assumed to be an ideal gas with constant coefficient  $\gamma$  equal to 1.4 and standard density  $\rho_0$  equal to  $1.293 \text{ kg/m}^3$ . High explosive TNT is modelled with a Mie-Grüneisen equation of state and the Jones-Wilkins-Lee [18] formalism for the reference curve, with related parameters given in table 1. Stations are positioned all around the external faces of the structure and register the applied pressure history under blast. The density of the stations is increasing with charge proximity, in order to capture detailed signals next to the charge. Pressure histories are registered until the air shock wave has totally diffracted around the structure and no more significant overpressure is applied to the structure.

**Table 1:** Parameters Mie-Grüneisen and JWL for TNT

Parameter	a (GPa)	b (GPa)	$R_1$ -	$R_2$ -
Value	3395	82	8.3	2.8
Parameter	$\omega$ -	$\rho_0$ ( $\text{kg/m}^3$ )	$P_{CJ}$ (GPa)	$D_{CJ}$ (m/s)
Value	0.6	1645	18	6930

#### Stage 3: dynamic response under blast

The dynamic response of the structure is calculated with ABAQUS Explicit from detonation time to 50 ms, which is a sufficient step time to capture the complete response to the blast. The pressure applied on the external face of a finite element is the signal of the closest Eulerian station in the blast load calculation.

#### Stage 4: post-blast capacity assessment

The residual axial bearing capacity of the blast-damaged column is evaluated with a quasi-static ABAQUS Explicit calculation. A vertical downward force is gradually applied on the top of the column with the bottom fixed, until failure is reached. As proposed by Shi *et al.* [10] and detailed in equation 1, the damage index  $D$  is related to the ratio between the reduced capacity of the blast-damaged column  $P_{residual}$  and the nominal capacity of the

component  $P_{nominal}$ .

$$D = 1 - \frac{P_{residual}}{P_{nominal}} \quad (1)$$

### 3 VALIDATION OF THE ANALYTICAL PROCEDURE

#### 3.1 Close-in detonation tests on RC components

The numerical damage assessment of a two-third scale RC column ( $0.4 \times 0.4 \times 2.4 \text{ m}^3$ ) subjected to close-in detonation is compared with the experimental test reported by Wu *et al.* [12]. In this test, the column is placed horizontally between a top head and a foundation block, so that the ground acts as lateral support. It is subjected to the detonation of a parallelepiped charge equivalent to 25 kg of TNT at a standoff distance of 200 mm.

Figure 3a shows a photograph of the column after the blast which sustained severe damage around the region of the explosive charge; concrete is totally crushed, longitudinal reinforcement bars suffered large lateral deformation and transverse reinforcement bars shifted largely from their initial locations.

The numerical result is shown in figure 3b, where colour fringes indicate the maximum tensile strain in concrete. The computed crack profile of concrete, as well as the large lateral deformations of longitudinal and transverse reinforcement are correctly reproduced.

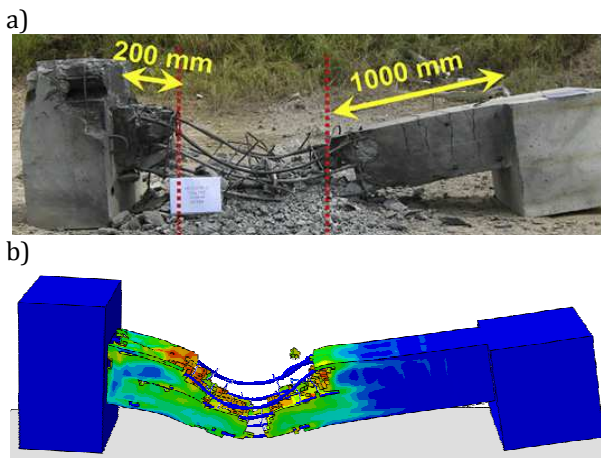


Figure 3: Detonation near a RC column

a) experimental and b) numerical results

Numerical damage assessments of RC slabs subjected to close-in detonation were compared with a set of experimental tests performed by CEA-Gramat.

Figure 4a shows the result of the detonation a 1 kg charge at a distance of 6 cm from a  $1.4 \times 1.4 \times 0.1 \text{ m}^3$  slab. At the back face, a quasi-circular hole and a spall are observed in concrete, with respective average diameters of 16 and 45 cm. At the centre of the slab, reinforcement bars suffered such large deformations that some of them are broken.

Figure 4b shows the numerical results with separated view of plastic deformations in steel and damage distribution in concrete. Experimental details are properly reproduced, even if the fully damaged part of concrete is not yet totally separated from the rest of the slab at the end of the calculation.

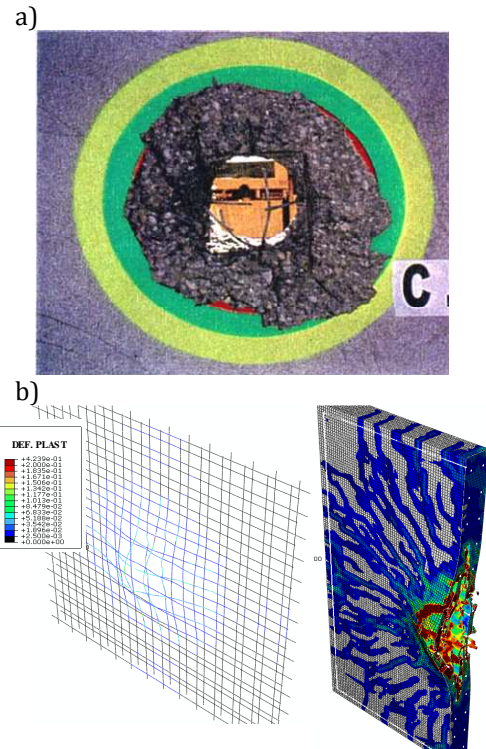


Figure 4: Detonation near a RC slab  
a) experimental and b) numerical result



### 3.2 Axial compressive capacity of a RC column

The methodology for assessing axial bearing capacity of columns is validated on undamaged columns. The maximum load capacity of columns obtained from quasi-static axial compressive calculations is compared to the nominal capacity given by the Mac Gregor [19] and ACI formula. According to this formula given by equation 2, the maximum axial carrying capacity of an undamaged RC column  $P_N$  depends on the concrete compressive strength  $\sigma_c$ , the longitudinal reinforcement yield strength  $\sigma_y$ , the gross area of the column cross-section  $A_G$  and the area of the longitudinal reinforcement  $A_S$ .

$$P_N = 0.85\sigma_c (A_G - A_S) + \sigma_y A_S \quad (2)$$

For all relevant columns of the generic building, deviations are found to be less than 5% between the nominal strengths obtained by the Mac-Gregor and ACI code formula and by the ABAQUS quasi-static calculations.

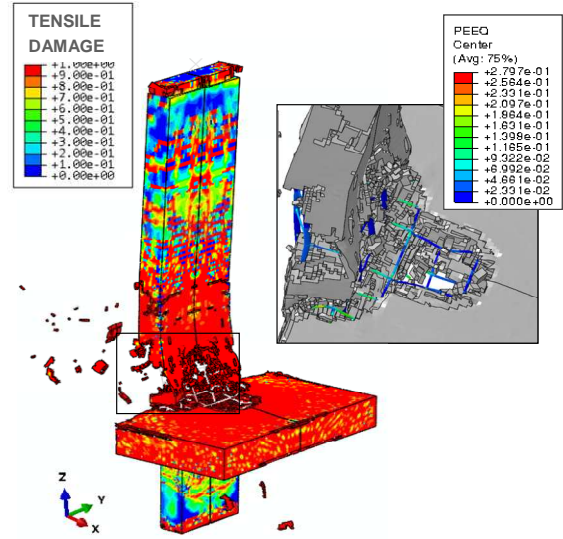
## 4. NUMERICAL RESULTS

### 4.2 Simulations of explosive scenarios in a generic building

Within the SPIRIT project, a total of 14 scenarios of near field or contact explosive attacks from 2.5 to 500 kg equivalent TNT on a modern high-rise generic building have been derived.

Figure 5 shows the numerical results for 25 kg TNT in contact with a column-to-slab corner at the third floor of the building (scenario 1). The distribution of tensile damage in concrete (0 for undamaged and 1 for fully damaged material) and plastic strains in steel reinforcement are represented. Concrete is severely damaged in both the column and the slab, with breaches formed. Large plastic deformations up to 27% are observed in steel. In that case, it is concluded that the column has no more residual axial capacity and is considered as a “missing” component for the analysis of the post-blast

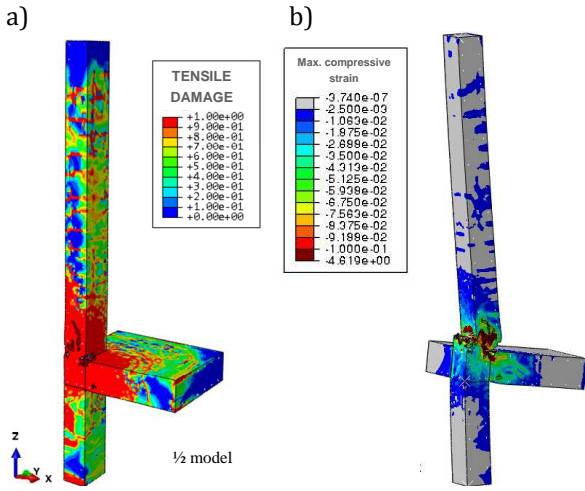
global stability of the building.



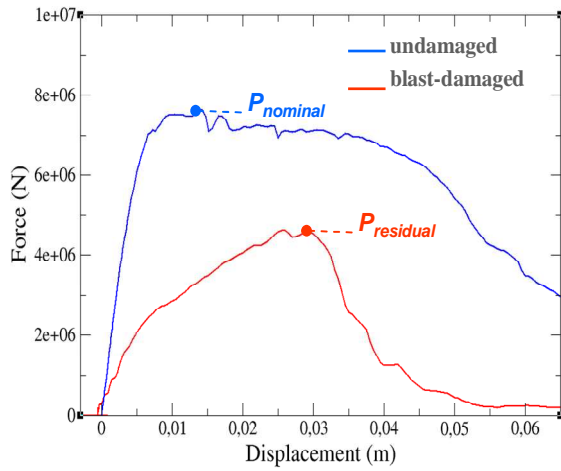
**Figure 5:** Damage in concrete and plastic strain in steel after blast in scenario 1

Figure 6a shows the numerical result for 2.5 kg TNT in contact with a column-to-slab corner at the sixth floor of the building (scenario 2). Concrete clearly suffered high damage next to the charge in both the column and the slab, as well as in several horizontal sections in the upper part of the column, due to bending actions. However, only small parts of concrete are eroded in front of the charge and at the rear faces of the column and the slab. In that case, a post-blast compressive calculation is performed. The result is shown on figure 6b which represents the maximal compressive strain distribution. The column clearly failed in the section which was the most damaged by the blast.

On figure 7 are plotted the applied axial compressive force versus downward displacement during the compressive calculation, on which elastic, plastic, and softening stages are captured. The comparison of curves obtained on the undamaged and blast-damaged column clearly points out the degradation of the initial stiffness and maximum load capacity of the column previously damaged by the blast. In that case, a damage index of 36% is deduced.



**Figure 6:** a) Damage in concrete after blast and b) Maximum strain in concrete after compression test for scenario 2



**Figure 7:** Axial force versus displacement during numerical compressive test of scenario 2.

#### 4.2 Parametric simulations for the numerical experiment plane

In order to broaden the assessment of explosion scenarios in a generic building to a larger number of situations, a parametric analysis is performed. In these simulations, the detailed fluid dynamic eulerian calculation of the blast load is substituted by the use of the Conwep module in ABAQUS, which requires less computing time. This module computes from tabulated data of TM5-1300 Technical Manual [11] the blast loading histories depending of the charge weight, the standoff distance and the orientation of the loaded surface. The response of a RC column under near field detonation with the pressure loading

computed by the Conwep module has been compared with the response obtained using the eulerian 3D simulation for the blast loading. The comparison showed reasonable agreement on the damage distribution in concrete due to the blast and on the residual axial compressive strength of the column after blast, even if the results obtained with Conwep are more conservative.

Table 2 lists the parameters considered in the plane of numerical experiments of near field detonations on RC columns. The parameters under consideration include the compressive strength of concrete  $\sigma_c$ , the column thicknesses along the charge direction  $t$ , a dimensionless parameter  $w/t$  which is the ratio between the column width  $w$  and the column thickness  $t$ , the column height  $H$ , the charge radius  $R$  and a dimensionless parameter  $d/R$  which is the ratio between the standoff distance  $d$  to the charge radius  $R$ . The tensile strength is taken equal to one tenth of the compressive concrete strength and the longitudinal reinforcement ratio is taken constantly equal to 1.0 %.

**Table 2:** Parameters of the numerical experiment plane

Parameter	Values	Values			
		1	2	3	4
1 Section ratio	$w/t$	1.0	2.0		
2 Compressive strength	$\sigma_c$ (MPa)	25	35	50	
3 Column height	$H$ (m)	3.3	4.6	6.6	
4 Column thickness	$t$ (m)	0.25	0.35	0.5	
5 Charge radius	$R$ (m)	0.07	0.11	0.15	0.25
6 Relative distance	$d/R$	1.25	1.6	2.0	4.0

As the full combination of all these parameters would lead to 864 possible numerical simulations, a restricted number of 30 experiments have been done. This number is considered enough to extract a formula able to describe with a reasonable accuracy the influence of each parameter on the resulting damage level.

## 5. EMPIRICAL FORMULA TO PREDICT THE DAMAGE INDEX OF A COLUMN

### 5.1 Derivation of the formula

The results from the parametric analysis are used to establish an analytical formula that quantifies the column damage level  $D$  depending on the blast load and column characteristics. The formula takes the form given by equation 3.

$$\begin{aligned}
 D = & b_0 + [b_{11} \text{ or } b_{11}] \\
 & + [b_{21} \text{ or } b_{22} \text{ or } b_{23}] \\
 & + [b_{31} \text{ or } b_{32} \text{ or } b_{33}] \\
 & + [b_{41} \text{ or } b_{42} \text{ or } b_{43}] \\
 & + [b_{51} \text{ or } b_{52} \text{ or } b_{53} \text{ or } b_{54}] \\
 & + [b_{61} \text{ or } b_{62} \text{ or } b_{63} \text{ or } b_{64}] \quad (3)
 \end{aligned}$$

$b_{ij}$  are coefficients related to each of the  $i=1$  to 6 parameters and to the  $j = 1$  to 2, 3 or 4 possible values of each parameter (see table 2), which values are given in equation 4. These coefficients have been deduced from the results of the plane of numerical experiments, from which six experiments have been rejected in order to get a better accuracy of the formula.

The choice of each coefficient depends on the value considered for the associated variable. For instance, for an experiment with the following parameters  $w/t=1$ ,  $\sigma_c=25$  MPa,  $H=6.6$  m,  $t=0.25$  m,  $R=0.1099$  m and  $d/R=4$ , coefficient  $b_{11}$  has to be chosen as  $w/t$  takes value  $n^{\circ}1$  (equal to 1), coefficient  $b_{21}$  is chosen as second parameter because  $\sigma_c$  also takes value  $n^{\circ}1$  (equal to 25 MPa). Using the same methodology for other coefficients, damage parameter  $D$  finally equals to:

$$D = b_0 + b_{11} + b_{21} + b_{33} + b_{41} + b_{52} + b_{64}.$$

For values of the parameters which are different from the one defined in table 2,  $D$  can be obtained using linear interpolation or extrapolation of the coefficients  $b_{ij}$ . However, in case of extrapolation, it is recommended to remain inside a reasonable range ( $\pm 0.5$  time the variable interval of the experiment plane).

$$\begin{aligned}
 b_0 &= 0.692 \\
 b_{11} &= -0.007, b_{12} = 0.007 \\
 b_{21} &= 0.06, b_{22} = -0.038, b_{23} = -0.022 \\
 b_{31} &= 0.02, b_{32} = -0.029, b_{33} = -0.049 \\
 b_{41} &= 0.143, b_{42} = 0.074, b_{43} = -0.217 \\
 b_{51} &= -0.313, b_{52} = 0.109, b_{53} = 0.089, b_{54} = 0.175 \\
 b_{61} &= 0.103, b_{62} = 0.095, b_{63} = 0.017, b_{64} = -0.214 \quad (4)
 \end{aligned}$$

### 5.2 Accuracy of the formula

The accuracy of the mathematical formula can be checked by comparing its results with the results given by the thirty numerical simulations. For the 24 simulations used to establish the formula, the mean difference is less than 5 % and the maximum difference is equal to 15%,. If all the 30 numerical simulations are included, the mean difference is closed to 10 %. This accuracy is considered reasonable.

### 5.3 Effects of relevant parameters

Among the six parameters examined in the plane of experiments, the thickness of the column  $t$ , the charge radius  $R$  and the ratio of standoff distance to charge radius  $d/R$  prove to be the most significant on the column response. In fact, column with greater thickness implies more concrete area and larger cross-section, which results in an increase in both the shear and bending strengths. Variations of distance to charge radius ratio below 1.6 appear to have less effect on the damage level of the column than for higher ratios. This result seems to indicate a threshold effect in the local damage induced by detonations occurring at very low scaled distance from the column.

The column width  $w$ , the column height  $H$  and the concrete compressive strength  $\sigma_c$  do not play an important role. Increasing the width by a factor of two decreases very slightly the damage resistance of the column. This can be due to an increase in the blast loads acting on a wider column although shear and bending strength is constant. The non-significant effect of column height can be



explained by the damage mechanisms involved in these close-in detonations, which are mainly governed by local response of the material and cross-section erosion. The effect of  $\sigma_c$  was expected to be more important. The reason is probably linked to the dynamic concrete behavior under high pressure level. For such loading, the structure response is mainly governed by inertia and confinement effects which are probably an order of magnitude bigger than the compressive material strength.

## 6. CONCLUSIONS

In this work, a numerical procedure is proposed to simulate the behavior of RC structures under contact to near field detonation, and to estimate their residual bearing capacity. This procedure is used to quantify the local damage of structural components in several scenarios of explosive attacks in a generic residential building. Using a plane of numerical experiments the results are extended to more general configurations covering a significant number of situations encountered in existing or new buildings. From this parametric study, the effects of column dimension, concrete strength as well as charge size and standoff are investigated. An analytical formula that quantifies the column damage level as a function of the varying parameters is also extracted.

## 7. ACKNOWLEDGEMENTS

This work is performed within the 7th Framework program of the European Union. The progress of the project, called SPIRIT (Safety and Protection of built Infrastructure to Resist Integral Threat), can be followed on [www.infrastructure-protection.eu](http://www.infrastructure-protection.eu).

## REFERENCES

- [1] United States General Services Administration, 2004. Progressive collapse analysis and design guidelines for new federal office buildings and major modernization projects. Washington DC.
- [2] Department of Defense, 2009. Design of buildings to resist progressive collapse. *Unified Facilities Criteria 4-023-03*. Washington DC.
- [3] Marjanishvili, S. 2004. Progressive analysis procedure for progressive collapse. *J. Perform Constructed Facilities ASCE*. **18**:79-85.
- [4] Kaewkulchai, G. and Williamson, E. B., 2004. Beam element formulation and solution procedure for dynamic progressive collapse analysis. *Computers & Structures*. **82**:639-651.
- [5] Tsai, M. and Lin, B., 2008. Investigation of progressive collapse resistance and inelastic response for an earthquake-resistant RC building subjected to column failure. *Engineering Structures*. **30**:3619-3628.
- [6] Shi, Y., Li, Z.X. and Hao, H., 2010. A new method for progressive collapse analysis of RC frames under blast loading. *Engineering Structures*. **32**:1691-1703.
- [7] Li, Q. and Meng, H., 2002. Pulse loading shape effects on pressure-impulse diagram of an elastic-plastic, single-degree-of-freedom structural model. *Int. J. Mech. Sci.* **202**(44):1985-1998.
- [8] Fallah, A. and Louca, L., 2007. Pressure-impulse diagrams for elastic-plastic-hardening and softening single-degree-of-freedom models subjected to blast loading. *International Journal of Impact Engineering*. **34**:823-842.
- [9] Krauthammer, T., Astarlioglu, S., Blasko, J., Soh, T. and Ng, P., 2008. Pressure-impulse diagrams for the behavior assessment of structural components. *International Journal of Impact Engineering*. **35**:771-783.
- [10] Shi, Y., Hao, H. and Li, Z.X, 2008. Numerical derivation of pressure-impulse diagrams for prediction of RC column damage to blast load. *International Journal of Impact Engineering*. **35**:1213-1227.
- [11] TM5-1300, 1969. Structure to resist the effect of accidental explosions. Department of the army, Navy and Air Force.
- [12] Wu, K.C., Li, B. and Tsai, K.C., 2011. Residual axial compression capacity of

- localized blast-damaged RC columns. *International Journal of Impact Engineering*. **38**:29-40.
- [13] Pontiroli, C., Rouquand, A. and Mazars, J., 2010. Predicting concrete behaviour from quasi-static loading to hypervelocity impact: an overview of the PRM model, *European Journal of Environmental and Civil Engineering*. **14**(6-7):703-727.
- [14] Krieg, R.D., 1978. A simple constitutive description for soils and crushable foams, Sandia National Laboratories, SC-DR-72-0833, Albuquerque, New Mexico.
- [15] Swenson, D.V. and Taylor, L.M., 1983. A finite element model for the analysis of tailored pulse simulation of boreholes. *International Journal of Numerical and Analytical Methods in Geomechanics*. **7**:469-484.
- [16] Hillerborg, A., Modeer, M. and Petersson, P.E., 1976. Analysis of crack formation and growth in concrete beams of fracture mechanics and finite element. *Cement and Concrete Research*. **6**:773-782.
- [17] Jourden, H., Sibeaud, J-M. and Adamczewski-Cauret M., 1995. Logiciel OURANOS : présentation générale et utilisation en détonique. *Revue Scientifique et technique de la Défense*. **4**:51-58.
- [18] Lee, E.L., Hornig, H.C. and Kury, J.W., 1968. Adiabatic expansion of high explosive detonation products, Laurence Radiation laboratory, University of California.
- [19] Mac-Gregor, J.G.G., 1997. Reinforced concrete: mechanics and design. *Professional technical reference*. Englewood Cliffs, NJ: Prentice-Hall.